JOURNAL OF THEORETICAL
AND APPLIED MECHANICS
63, 3, pp. 691–700, Warsaw 2025
https://doi.org/10.15632/jtam-pl/205727

IMPACTS OF IMPLEMENTING STOCHASTIC EXCITATION TO ASSESS ANOMALIES ON RAILWAY VEHICLE DYNAMIC MODEL

Péter FERENCZ[1*], Gergő FODOR[2]

[1] *Department of Railway Vehicles and Vehicle System Analysis, Faculty of Transportation Engineering and Vehicle Engineering, Budapest University of Technology and Economics, Budapest, Hungary*
[2] *Department of Applied Mechanics, Faculty of Mechanical Engineering, Budapest University of Technology and Economics, Budapest, Hungary*

*corresponding author, *ferencz.peter@kjk.bme.hu*

This paper investigates the effects of incorporating stochastic features into the simulation of a dynamic suspension system. The study is motivated by a real-world anomaly phenomenon observed in railway vehicles, where changes in the stiffness of rubber springs during operation can lead to irregular motion. A series of tests were conducted to characterize these stiffness variations and their dynamic behavior under stochastic excitation. Using a simplified, symmetrically structured model, the study demonstrates that such changes can initiate system anomalies, accelerating the deterioration of the system's technical state and potentially leading to a significant reduction in component lifetime.

Keywords: stochastic process; system anomaly; technical state deterioration; Euler–Maruyama technique.

1. Introduction

Railway vehicle dynamics are profoundly influenced by the mechanical properties and performance of suspension components. In this study, we investigate a specific anomaly in the secondary suspension system of an electric locomotive type. In practice, intensive asymmetric wheel profile wear appeared during the long-time operation of these types of vehicles (Ferencz, 2010), meaning that the wheels on one side were subjected to larger degradation than on the other side of one wheelset. The problem originated from deviations in the stiffness properties of the suspension's rubber-to-metal spring (secondary spring) components, which were identified as the primary cause of the anomaly (Ferencz, 2010).

First, we explain the secondary spring measurements and their outcomes, then the six-degree-of-freedom mechanical model of the railway vehicle is introduced. We add independent track excitations on the left and the right side of the vehicle to include track irregularities, and thus the mathematical model of the system is a stochastic differential equation (SDE), as similarly used by Bruni *et al.* (2011) and Knothe and Stichel (2017).

Numerical techniques are used to simulate the motion of the vehicle, and from the simulation results we calculate the deformation distribution of the secondary springs during the steady-state

Ministry of Science and Higher Education
Republic of Poland

The publication has been funded by the Polish Ministry of Science and Higher Education under the Excellent Science II programme "Support for scientific conferences".
The content of this article was presented during the 40th Danubia-Adria Symposium on Advances in Experimental Mechanics, Gdańsk, Poland, September 24–27, 2024.

operation. Based on this distribution we can calculate the probability of critical operation (PCO) if we define a certain critical limit of operation (CLO). This critical limit in our case is a large secondary spring deformation we consider to be harmful and that might cause degradation and failure in the stiffness characteristics.

If the secondary spring stiffness changes due to critical operation, the model is not symmetric anymore. We show that in terms of PCO values the emerging asymmetric secondary spring structure is much more dangerous than a symmetric structure.

2. The subject

2.1. Suspension component tests

Anomalies in the suspension system parameters of railway vehicle structures (such as unexpected deviations between the secondary springs) can lead to unexpected reductions in component lifespan and accelerated deterioration of the system's technical condition.

In 2006, a detailed analysis was conducted on a set of layered rubber-to-metal spring units to evaluate their vertical stiffness characteristics after a significant number of system anomalies, e.g., asymmetric wheel wear was observed in practice. To further investigate the long-term behavior of these springs, new measurements were carried out in 2024 (as illustrated in Fig. 1). The analysis included units still in operation and others dismantled after approximately 5–6 years of use.

Fig. 1. Test bench set to measure spring characteristics.

The results revealed significant deviations in the stiffness parameters of the tested secondary spring components.

The measured stiffness characteristics were evaluated using the classical least squares regression method, providing statistical representations of the data. On the basis of the optimization parameters an average function can be calculated as drawn with red line. These characteristics could be compared to the nominal design characteristics (as illustrated in Fig. 2) drawn black, with the approach assumption that the spring units were accepted with prescribed tolerances at operation start time according to the assembly by manufacturer technical requirements.

The tested spring units that had been in operation for 5–6 years show substantial deviations in stiffness, particularly at the nominal design load point at displacement of 4 mm.

In the figure two units showed unexpectedly softness, considered as outliers due to a possible material defect. Leaving out these from the further calculations a corrected average function was obtained. The range of the considered calculated spring stiffness values is as follows:

$$r = \max\{s_i\} - \max\{s_i\} = 16.137\,\frac{\text{kN}}{\text{mm}} - 10.175\,\frac{\text{kN}}{\text{mm}} = 5.9622\,\frac{\text{kN}}{\text{mm}}. \tag{2.1}$$

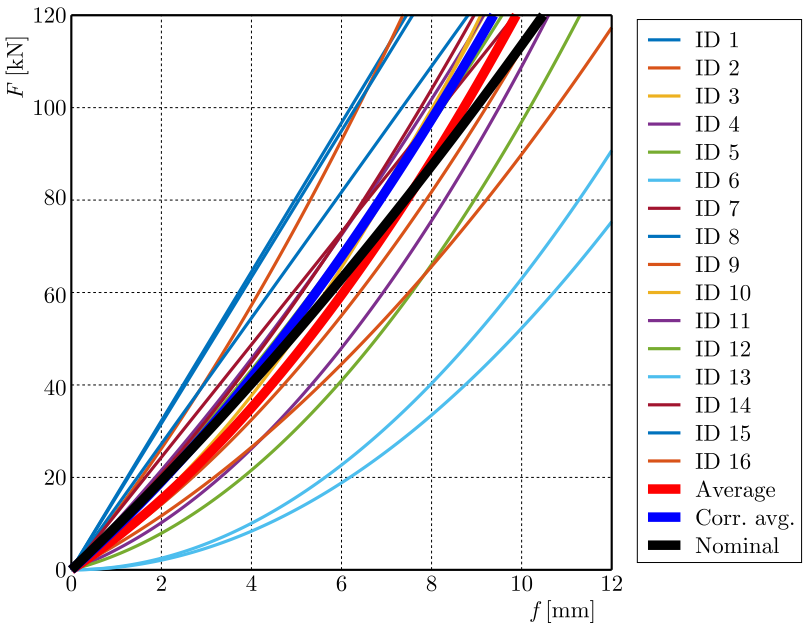

Fig. 2. Calculated vertical spring stiffness characteristics based on the measurements.

Statistical data from these measurements were incorporated into the mechanical model presented in Section 3, along with the specific mass and moment of inertia values of the locomotive under study.

2.2. System anomaly

An anomaly is when a certain system parameter exceeds its permitted in-operation maximum or minimum limit. From the measurements we conclude that during operation the secondary spring characteristics change due to such anomalies in the system. In the next section, we introduce a mechanical model of railway vehicles with random track ("road" contact surface) excitation that aims to explain an anomaly regarding the deformation of the secondary springs.

The actual phenomena can be described by the stochastic deterioration process $D(t, w)$ curve shown in Fig. 3. The curve shows with increasing operation time an increasing standard deviation banding around the expectation function indicated by $ED(t, w)$. It describes the natural physical process of normal material and structural damage, as the stochastic process of deterioration, as shown in Fig. 3 (Ferencz, 2023) over the time axis.

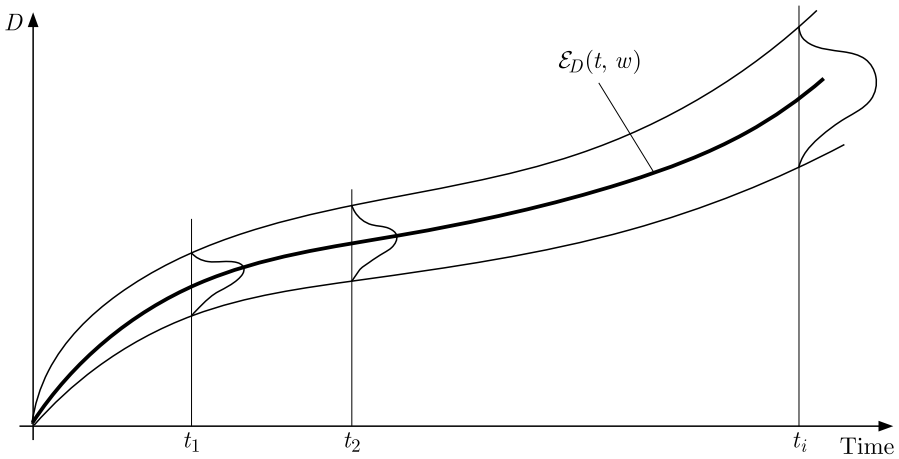

Fig. 3. Band characteristics of the deterioration process vs. time.

The natural degradation of spring stiffness change can be considered accordingly. Possible individual realization curves running within the bandwidth consist of two main sections divided by an inflexion point. The estimated speed of technical condition deterioration is exactly defined by the time-derivative process of $D(t, w)$, that depends on time t and on the elementary event w.

3. The mechanical model

In this study, a simplified six-degree-of-freedom mechanical model is utilized. The model as shown in Fig. 4, represents the cross section of the railway vehicle with three mass elements: half of a bogie and a quarter of a carbody structure over one wheelset.

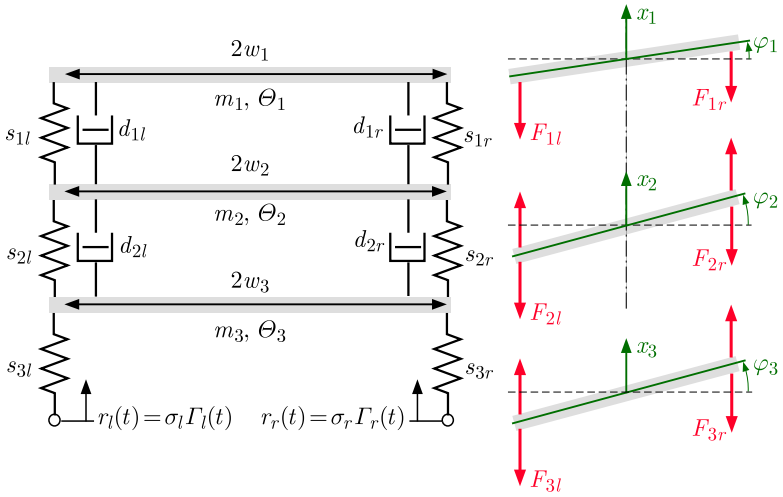

Fig. 4. Mechanical model.

The s parameters are spring stiffnesses, the d parameters represent damping, m, Θ and w are the mass, mass moment of inertia and half width of the different bodies, respectively. We presented the forces acting between the bodies on the right side of Fig. 4. The model focuses only on the behavior of the three components (half of a bogie and a quarter of a carbody structure over one wheelset) subjected to stochastic track excitation denoted by $r_l(t)$ and $r_r(t)$ (directly impacting the wheels) to highlight the statistical features and possible threats during operation.

The track excitation represents the irregularities of track rail lines on each side. The state vector is taken as follows: $\mathbf{y} = [x_3\ \dot{x}_3\ \varphi_3\ \dot{\varphi}_3\ x_2\ \dot{x}_2\ \varphi_2\ \dot{\varphi}_2\ x_1\ \dot{x}_1\ \varphi_1\ \dot{\varphi}_1]^{\mathrm{T}}$. The vector elements are the considered movements and their derivatives as velocity parameters.

The probabilistic nature of the excitation is captured by two separate white noise processes: $W_l(t)$ on the left side and $W_r(t)$ on the right.

The following forces are acting on the bodies:

$$
\begin{aligned}
F_{1l} &= s_{1l}(x_1 - w_1\sin(\varphi_1) - x_2 + w_2\sin(\varphi_2)) + d_{1l}(\dot{x}_1 - \dot{\varphi}_1 w_1\cos(\varphi_1) - \dot{x}_2 + \dot{\varphi}_2 w_2\cos(\varphi_2)),\\
F_{1r} &= s_{1r}(x_1 + w_1\sin(\varphi_1) - x_2 - w_2\sin(\varphi_2)) + d_{1r}(\dot{x}_1 + \dot{\varphi}_1 w_1\cos(\varphi_1) - \dot{x}_2 - \dot{\varphi}_2 w_2\cos(\varphi_2)),\\
F_{2l} &= s_{2l}(x_2 - w_2\sin(\varphi_2) - x_3 + w_3\sin(\varphi_3)) + d_{2l}(\dot{x}_2 - \dot{\varphi}_2 w_2\cos(\varphi_2) - \dot{x}_3 + \dot{\varphi}_3 w_3\cos(\varphi_3)),\\
F_{2r} &= s_{2r}(x_2 + w_2\sin(\varphi_2) - x_3 - w_3\sin(\varphi_3)) + d_{2r}(\dot{x}_2 + \dot{\varphi}_2 w_2\cos(\varphi_2) - \dot{x}_3 - \dot{\varphi}_3 w_3\cos(\varphi_3)),\\
F_{3l} &= s_{3l}(x_3 - w_3\sin(\varphi_3)),\\
F_{3r} &= s_{3r}(x_3 + w_3\sin(\varphi_3)).
\end{aligned}
\tag{3.1}
$$

The stochastic track excitations are taken as

$$r_l(t) = \sigma_l \Gamma_l(t), \qquad r_r(t) = \sigma_r \Gamma_r(t), \tag{3.2}$$

where $\Gamma_l(t)$ and $\Gamma_r(t)$ represent independent white noise processes modeling the random irregularities of the track with noise intensities σ_l and σ_r on the left and right side, respectively. The equation of motion of the system is a stochastic differential equation (SDE) (Sun, 2006) written in an incremental form:

$$\mathrm{d}\mathbf{y} = \mathbf{f}(\mathbf{y})\,\mathrm{d}t + \mathbf{g_l}(\mathbf{y})\,\mathrm{d}W_l + \mathbf{g_r}(\mathbf{y})\,\mathrm{d}W_r, \tag{3.3}$$

where the elements of the deterministic part $\mathbf{f}(\mathbf{y})$ are as follows:

$$\begin{aligned}
f_1(\mathbf{y}) &= \dot{x_1}, & f_2(\mathbf{y}) &= -g + \frac{1}{m_1}(-F_{1l} - F_{1r}),\\
f_3(\mathbf{y}) &= \dot{\varphi_1}, & f_4(\mathbf{y}) &= \frac{1}{\Theta_1}(F_{1l} - F_{1r})w_1\cos(\varphi_1),\\
f_5(\mathbf{y}) &= \dot{x}_2, & f_6(\mathbf{y}) &= -g + \frac{1}{m_2}(-F_{2l} - F_{2r} + F_{1l} + F_{1r}),\\
f_7(\mathbf{y}) &= \dot{\varphi_2}, & f_8(\mathbf{y}) &= \frac{1}{\Theta_2}(F_{2l} - F_{2r} - F_{1l} + F_{1r})w_2\cos(\varphi_2),\\
f_9(\mathbf{y}) &= \dot{x_3}, & f_{10}(\mathbf{y}) &= -g + \frac{1}{m_3}(-F_{3l} - F_{3r} + F_{2l} + F_{2r}),\\
f_{11}(\mathbf{y}) &= \dot{\varphi_3}, & f_{12}(\mathbf{y}) &= \frac{1}{\Theta_3}(F_{3l} - F_{3r} - F_{2l} + F_{2r})w_3\cos(\varphi_3).
\end{aligned} \tag{3.4}$$

The stochastic effects of the track excitation are given on the left side by the vector $\mathbf{g_l}(\mathbf{y})$ and the corresponding Wiener-process increment $\mathrm{d}W_l$, and on the right side $\mathbf{g_r}(\mathbf{y})$ and $\mathrm{d}W_r$. The elements of the vectors are

$$\begin{aligned}
g_{l10}(\mathbf{y}) &= -\frac{s_{3l}}{m_3}\sigma_l, & g_{l12}(\mathbf{y}) &= \frac{s_{3l}}{\Theta_3}w_3\sigma_l\cos\varphi_3,\\
g_{r10}(\mathbf{y}) &= -\frac{s_{3r}}{m_3}\sigma_r, & g_{r12}(\mathbf{y}) &= -\frac{s_{3r}}{\Theta_3}w_3\sigma_r\cos\varphi_3.
\end{aligned} \tag{3.5}$$

The not listed elements of $\mathbf{g_l}(\mathbf{y})$ and $\mathbf{g}_r(\mathbf{y})$ are zeros. The $\mathrm{d}W_l$ and $\mathrm{d}W_r$ increments are random variables of independent normal distributions with zero expected values and $\mathrm{d}t$ variance. The system's behavior is investigated based on numerical simulations.

4. Results

Our main interest lies in understanding what happens with the secondary springs (characterized by s_{1l} and s_{1r} on the left and right sides below the carbody) during long-time operation. For that, relatively long simulations are performed to have enough data to estimate the steady-state distribution of the deformation (length change) Δl in the springs. The deformation is calculated at each time step from the state variables:

$$\Delta l = \sin(\varphi_2)w_2 - \sin(\varphi_1)w_1. \tag{4.1}$$

In expectation, the springs are compressed by about 4 mm nominally. The Δl is the deformation of the left secondary spring about this expected compression value. Note that the deformation of the right secondary spring would be $-\Delta l$. From the simulations we can calculate the distribution of this deformation during the steady-state operation. If we set a critical limit of operation (CLO), which means that at certain deformation the springs are subjected to weakening or potential failure, we can calculate the probability of critical operation (PCO) in the steady state.

4.1. Simulations

In practice, SDEs are investigated mainly utilizing numerical solvers, since exact analytical solutions only exists for a handful of simple examples.

The simulations presented in this paper are acquired by using an implicit Euler–Maruyama scheme built into the DifferentialEquations.jl package of The programming language Julia. Explicit schemes struggle to converge properly for stiff problems, and since the spring stiffnesses are large in our system, the performance of implicit schemes is much better (Rackauckas & Nie, 2020).

First, we consider the system to be symmetric, i.e., $s_{1l} = s_{1r} = s_1$, $d_{1l} = d_{1r} = d_1$, $s_{2l} = s_{2r} = s_2$, $d_{2l} = d_{2r} = d_2$, $s_{3l} = s_{3r} = s_3$, and $\sigma_l = \sigma_r = \sigma$. Only the noise processes differ on the two sides. In this case, the simulations are carried out using the parameters in Table 1. This study focused on the variability of the stiffness parameters. It is to be mentioned that the energy dissipation characteristics of these spring units after a certain deteriorated technical state are an object of further investigations. Table 1 shows special damping parameter figures cited from calculations of the certain locomotive type structural nominal design parameters (Ferencz, 2010). The indicated stiffness values were by purpose chosen to avoid possible numerical distortion in the solver process. With this possibility, the influence of the noise and the real asymmetricity of the focused secondary suspension system elements could be qualitatively examined.

Table 1. Simulation system parameters.

Parameter	Value	Unit	Parameter	Value	Unit	Parameter	Value	Unit
m_1	10450	kg	m_2	4305	kg	m_3	3640	kg
Θ_1	104 250	$\mathrm{kg \cdot m^2}$	Θ_2	8 610	$\mathrm{kg \cdot m^2}$	Θ_3	7280	$\mathrm{kg \cdot m^2}$
w_1	1	m	w_2	1	m	w_3	1	m
s_1	12 746 000	N/m	s_2	1 035 000	N/m	s_3	2 070 000	N/m
d_1	1409	Ns/m	d_2	2000	Ns/m	σ	0.001	1

Figure 5 shows the simulation results of state variables over time in relation to their respective expected solutions. The expected solution is when the noise is removed from the system in this

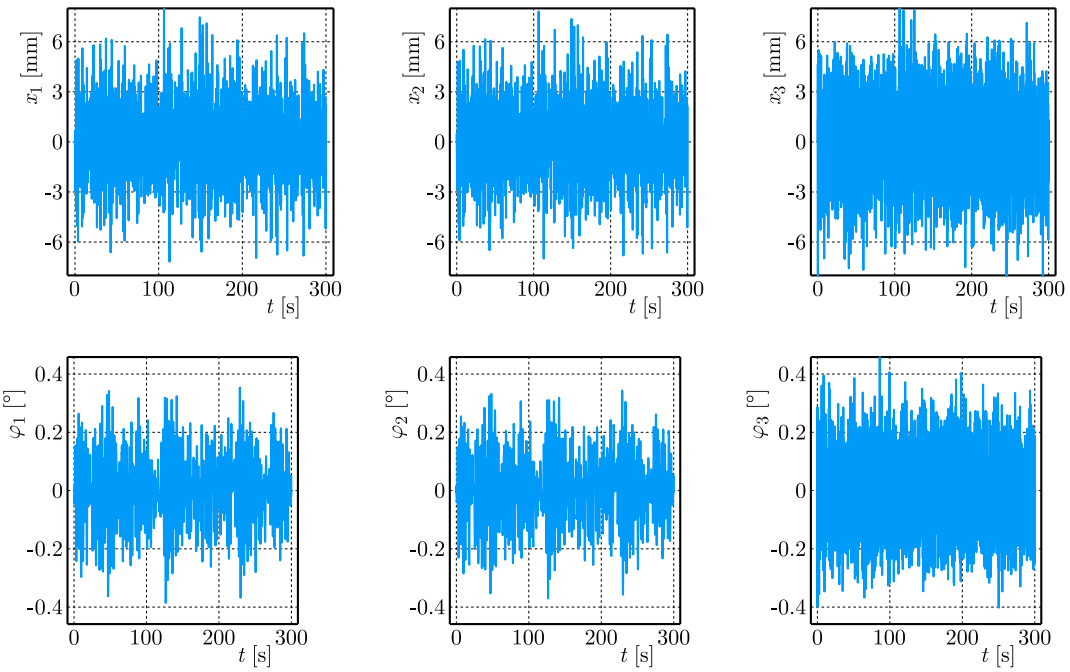

Fig. 5. Simulations results of state variables, plotted about their steady-state solution.

case. For example, the expected solution of the rotational movement angles of the bodies φ_1, φ_2, φ_3 are zero, because the system is symmetric. However, the stochastic excitation forces the bodies to move randomly, and the rotational angles constantly deviate from the expected zero value.

4.2. Probability of critical operation (PCO)

Hypothetically an anomaly process can appear on the basis of an operation with critical considered parameters within the system. This acts as the necessary first criteria to exist and to step toward, to "detour the system" toward an anomaly process. To model this, we can use the empirical density function values of the spring characteristic features to calculate the secondary spring deformation Δl changes from the state variables in each time step. The distribution is shown in Fig. 6.

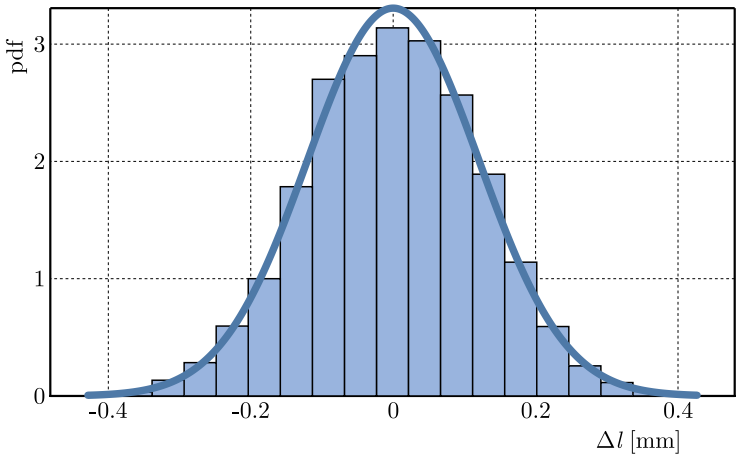

Fig. 6. Secondary spring deformation distribution during steady-state operation.

If we set a critical limit of operation (CLO), i.e., a $\pm\Delta l$ value for which the process is considered unsafe, we can calculate the PCO based on this distribution.

Figure 7 displays the connection between the CLO and the PCO values in the case of a symmetric secondary spring structure. For example, if we set the critical limit to zero, the probability that we have larger deformations is equal to 100 %. The larger CLO, the lesser gets PCO. According to the measurements explained in Section 2, there is a significant deviation in the secondary spring stiffness values s_1. We calculated the PCO for a symmetric case, when the secondary springs on the left and right sides are identical.

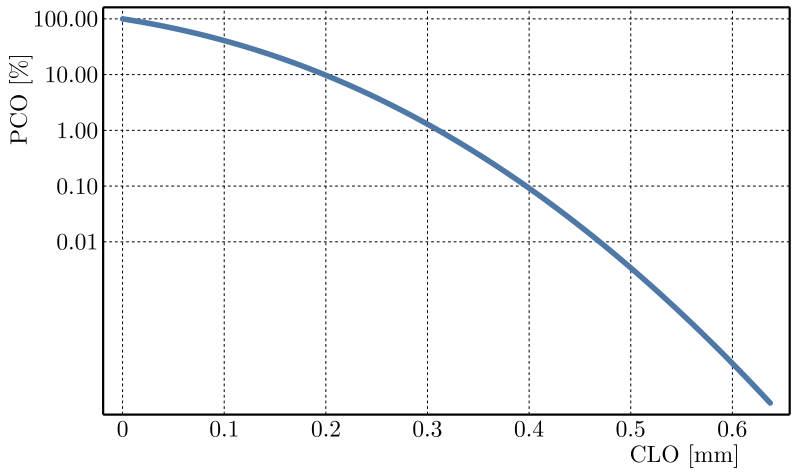

Fig. 7. Probability of critical operation (PCO) as a function of the critical limit of operation (CLO).

We considered two asymmetric cases: 1 % asymmetry means the s_{1r} is 99 % and s_{1l} is 101 % of the nominal value. Second, 5 % asymmetry is when s_{1r} is 95 % and s_{1l} is 105 %. Figure 8 shows the steady-state distribution of the secondary spring deformation Δl in the symmetric and asymmetric cases. In asymmetric cases the expected rotation movement angle of the carbody φ_1 is no longer zero, i.e., there is a steady-state tilt. If the expected value of φ_1 is not zero, then the expected value of Δl also differs from zero. Figure 8 displays how the Δl distributions shift depending on the measure of secondary spring asymmetry. For larger asymmetry values, the distribution is centered further aligned from zero value.

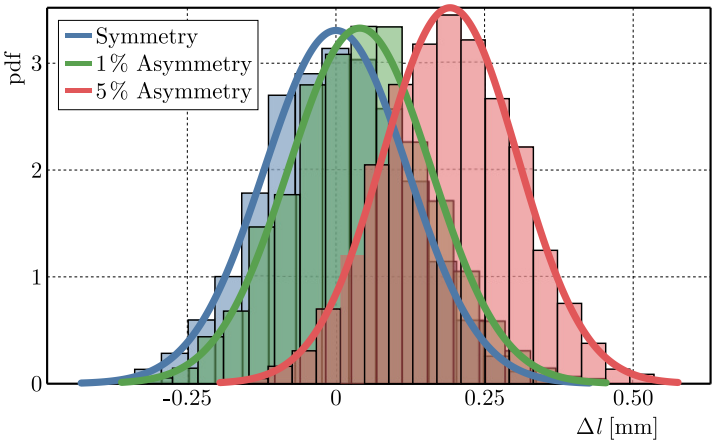

Fig. 8. Symmetric and asymmetric steady-state distribution of Δl.

Figure 9 presents the PCO values for the symmetric and asymmetric cases. For a certain CLO value, e.g., 0.4 mm, the symmetric probability is around 0.7 %, the 1 % asymmetric probability is slightly larger than 0.1 %, close to the symmetric case, but the 5 % asymmetric probability is more than 4 %. This essentially means that larger asymmetry causes high probability for the vehicle system itself to be in critical operation.

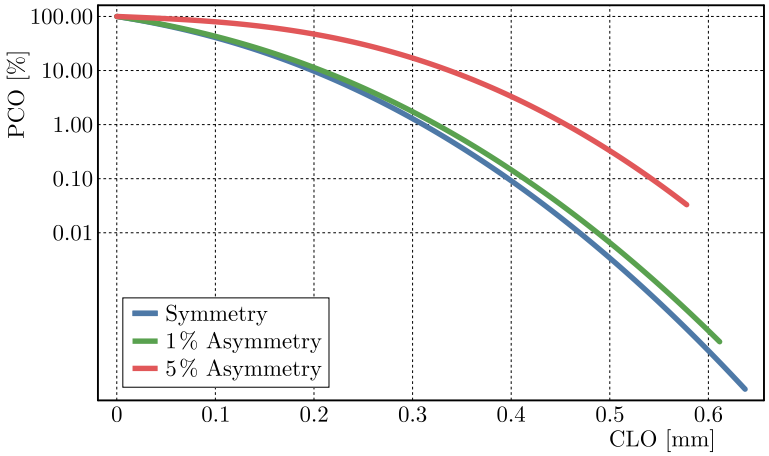

Fig. 9. PCO as a function of CLO for symmetric and asymmetric cases.

If we specify the operation time (OT) to be, e.g., 10000 hours, we can transform the PCO into critical operation time (COT):

$$\mathrm{COT} = \mathrm{PCO} \times \mathrm{OT}. \tag{4.2}$$

Table 2 presents the COT values for different cases. Note that as the CLO increases for a certain case, i.e., we allow larger deformation of these secondary springs, the COT values decrease. However, if we fix the CLO value at 0.5 mm and focus on the effect of asymmetry,

Table 2. COT in different cases.

	CLO [mm]	PCO [%]	COT [hours]
Sym	0.4	0.07	7.03
1 % Asym	0.4	0.107	10.7
5 % Asym	0.4	4.09	409.9
Sym	0.5	0.0022	0.22
1 % Asym	0.5	0.00426	0.426
5 % Asym	0.5	0.407	40.7

we see that out of 10000 hours the symmetric springs spend 0.22 hours in critical operation, which seems low, but the 5 % asymmetric springs spend 40.7 hours.

5. Conclusions

This paper provides an opportunity to assess the impacts of stochastic excitation on symmetrically and asymmetrically structured models of a railway vehicle. The results indicate that, even under nominal structural conditions, the system can exhibit anomalies when subjected to random forcing. The noise may drive the system into unexpected motions, especially during asymmetric operation conditions.

One can consider a symmetric case: the left and right secondary spring stiffness is the same. Even in a symmetric case the probability of critical operation is not zero in the presence of stochastic track excitation. After some time, one of the springs gets damaged due to operating above its intended limit. Its stiffness changes, and now the system is asymmetric because the stiffnesses of the secondary springs are different on the two sides. The PCO is larger in the asymmetric case, therefore the system spends even more time in critical operation than before, which means that an anomaly process develops with high probability.

Acknowledgments

Hereby as authors of this article, we express our special thanks to tutors Professor András Szabó, Professor Lajos Borbás, and Professor Vince Nagy.

References

1. Bruni, S., Meijaard, J., Rill, G., & Schwab, A.L. (2020). State-of-the-art and challenges of railway and road vehicle dynamics with multibody dynamics approaches. *Multibody System Dynamics*, *49*(1), 1–32. https://doi.org/10.1007/s11044-020-09735-z

2. Bruni, S., Vinolas, J., Berg, M., Polach, O., & Stichel, S. (2011). Modelling of suspension components in a rail vehicle dynamics context. *Vehicle System Dynamics*, *49*(7), 1021–1072. https://doi.org/10.1080/00423114.2011.586430

3. DifferentialEquations.jl: Efficient differential equation solving in Julia. https://docs.sciml.ai/DiffEqDocs/stable/

4. Ferencz, P. (2010). Investigation into wheel profile wear processes influenced by parameter anomalies in suspension characteristics of electro-locomotive bogies. In I. Zobory (Ed.), *Proceedings of the 8th International Conference on Railway Bogies and Running Gears* (pp. 201–212). Department of Rolling Stock, Budapest, Hungary.

5. Ferencz, P. (2023, September 26–29). *Investigation into impacts of dynamic system anomalies on railway vehicle wheel wear propagation* [Conference poster presentation]. 39th Danubia-Adria Symposium on Advances in Experimental Mechanics, Siófok, Hungary.

6. Knothe, K., & Stichel, S. (2017). *Rail vehicle dynamics*, Springer. https://doi.org/10.1007/978-3-319-45376-7

7. Rackauckas, C., & Nie, Q. (2020). Stability-optimized high order methods and stiffness detection for pathwise stiff stochastic differential equations. In *2020 IEEE High Performance Extreme Computing Conference (HPEC)*, Waltham, MA, USA, (pp. 1–8). https://doi.org/10.1109/HPEC43674.2020.9286178

8. Sun, J.Q. (2006). Stochastic dynamics and control. *Monograph Series on Nonlinear Science and Complexity* (vol. 4). Elsevier Science & Technology. https://doi.org/10.1016/S1574-6917(06)04001-3

9. The Julia Programming Language. https://julialang.org/

10. Zobory, I. (1997). Prediciton of wheel/rail profile wear. *Vehicle System Dynamics*, *28*(2–3), 221–259. https://doi.org/10.1080/00423119708969355

Manuscript received December 15, 2024; accepted for publication May 29, 2025; published online July 16, 2025.